Journal of Innovative Technology, Vol. 7, No. 1, pp. 99-116, March 2025
http://doi.org/10.29424/JIT.202503_7(1).0009

Numerical investigation for breast cancer risk model: An ODE based approach integrating body mass dynamics

Afshan Fida [1], Muhammad Asif Zahoor Raja [2*], Chuan-Yu Chang [3], Maryam Pervaiz Khan [4]

ABSTRACT

Breast cancer remains a leading cause of mortality among women worldwide, driven by a complex interplay of genetic, lifestyle, and physiological factors. Traditional risk assessment models rely on statistical parameters, limiting their predictive accuracy for breast cancer. This study aims to enhance predictive modeling by applying mathematical approaches, including ordinary differential equations (ODE's) based breast cancer risk model (BCRM), to understand the dynamics of body mass and its impact on cancer risk. We create sufficient large datasets to explore model robustness using methods like Adams' numerical solver, backward differentiation formula (BDF) method, explicit Runge-Kutta technique, and implicit Runge-Kutta method. The results are analyzed by comparing these four state-of-the-art numerical methods. Our findings highlight the strengths of these numerical methods, presenting solution plots and absolute error analyses to demonstrate the efficacy of the breast cancer risk model in capturing cancer risk trajectories and advancing diagnostic accuracy.

Keywords: Numerical Computing, Adams' numerical solver, Backward differentiation formula, Explicit and implicit Runge-Kutta method, Breast cancer risk model

1. INTRODUCTION

Breast cancer is a leading health concern worldwide, with incidence and mortality rates. Various risk factors like lifestyle choices, genetic predisposition, and body composition substantially influence health outcomes [1]. In the 21st century, cancer is the leading public health, economic and social problem [2]. Cancer is responsible for one in six deaths worldwide [3]. A significant portion of cancer diagnoses in women, the leading cause of cancer-related mortality globally in women is breast cancer. Breast cancer is the most common cancer among women worldwide. After lung cancer, the second leading cause of death among women is breast cancer [4]. Cancer is not a single disease; it's a collection of disorders that cause cells in the body to change and grow uncontrollably [5]. Categories of cancer are based on the type of fluid or tissue they originate from or by the area of the body where they initially develop [6]. Among other types of cancers, breast cancer is the most frequently diagnosed cancer in women [7], with an estimated 2.3 million new cases diagnosed globally each year [8]. Studies have shown that 5 to 10 percent of breast cancer can be ascribed to family history and genetic mutations, whereas 20 to 30 percent can be ascribed to modifiable reasons [9]. Its occurrence and mortality rates have risen over the past three decades. Breast cancer is a condition where abnormal cells in the breast multiply uncontrollably, leading to the formation of tumors. If not treated, tumors can spread to other parts of the body and become life-threatening [10-11].

The complexity of breast cancer has long been identified and investigated. Starting in the 1980's, the initial classification of the disease was based on microscopic tissue characteristics [12]. Breast cancers were initially classified based on estrogen receptor expression and later based on human epidermal growth factor receptor 2 (HER2) status [13]. By the turn of the millennium, the advent of microarray technology revealed that their mRNA expression profiles were linked to the phenotypic differences between breast cancer [14]. Magnetic resonance imaging (MRI), ultrasound, and mammography are different medical procedures commonly used in detecting and diagnosing breast cancer [15]. One powerful imaging tool that generates high-resolution images without the need to apply harmful radiation is MRI. This method resembles nuclear magnetic resonance, where a proton density image of the tissue is analyzed to produce an MRI image [16]. An x-ray picture of the breast is mammography [17]. In certain breast screening programs, digital mammography has taken the place of conventional mammography [18] because possible advantages of digital mammography include computer-aided detection. The use of computer-aided detection involves algorithm-based software that alerts radiologists to potential abnormalities in mammograms, enabling centralized interpretation of images [19].

The key risk factors have been recognized as body mass index (BMI) and obesity [20]. Studies show a positive correlation between increased body mass and increased breast cancer risk, especially among postmenopausal women [21]. Cancer risk remains

Manuscript received November 17, 2024; revised December 11, 2024; accepted January 7, 2025.

[1] Ph.D. Scholar, Graduate School of Engineering Science and Technology, National Yunlin University of Science and Technology, Taiwan, R.O.C.

[2*] Professor (corresponding author), Graduate School of Engineering Science and Technology, National Yunlin University of Science and Technology, Taiwan, R.O.C. (email: rajamaz@yuntech.edu.tw)

[3] Professor, Department of Computer Science and Information Engineering, National Yunlin University of Science and Technology, Taiwan, R.O.C.

[4] Ph.D. Scholar, Department of Computer Science and Information Engineering, Graduate School of Engineering Science and Technology, National Yunlin University of Science and Technology, Taiwan, R.O.C.

challenging despite capturing the dynamic interplay between body mass changes. Statistical parameters are most often used for traditional risk assessment models, which limit the prediction ability of risk breast cancer, to address this gap, there is a growing interest in applying mathematical modeling approaches like ordinary differential equations (ODE's) [22] to explain the complex ways in which body's systems interact and lead to cancer growth. The modern computing approaches are used by many researches in different areas of interest such as novel data approach for urbanized smart grids [23], fractional gradient-based optimized convolutional networks [24], clinical deep learning for C-section forecasting [25], interpolation scheme for CSMRI techniques [26], non-technical loss detection in smart grid [27], smoking prediction in hidden smokers [28], early diabetes detection [29], cost storage in wireless sensor using blockchain [30].

The brief interpretation of the findings and contributions of the study are as follows:

- This study explores breast cancer risk models by integrating body mass dynamics over time by applying the Adams numerical method, BDF method, explicit Runge-Kutta method, and implicit Runge-Kutta method.
- To create sufficient large datasets of numerical techniques to facilitate the comparison between Adams numerical and BDF methods, as well as between the explicit and implicit Runge Kutta methods to obtain intended results in the form of absolute error plots and solution plots.
- The purpose of this study is to produce approximate solutions of breast cancer risk model BCRM through modeling with ordinary differential equations (ODE's).
- Using Adam's solver, a synthetic dataset is mathematically created for the breast cancer risk model by changing the values of certain parameters, such as the logistic-growth rate of healthy breast cells, the rate of overflowing estrogen from DNA, the rate of immune suppression with estrogen, and the fat-carrying capacity rate.
- The analysis of absolute error plots and solution plots portrayed the robustness and effectiveness of the breast cancer risk model.

The rest of the paper is structured as follows: we formulate a mathematical modeling of the breast cancer risk model in section (2). The solution methodology is explained in section (3). The tabular and graphical illustration of results and discussion are shown in section (4). A concluding remark along with potentials of future path in breast cancer risk has been made in section (5).

2. MATHEMATICAL MODELING

Five-dimensional ordinary differential equations (ODE's) shown in equations (1-5) are considered to formulate a model. Here the significant risk factors of breast cancer are fat cells, as breast cancer is affected by the dynamics of fat cells. Here H(t) represents healthy cells, T(t) represents tumor cells, I(t) represents immune cells, E(t) represents effect of estrogen and F(t) represents fat cells, we will analyze the relationship between H(t), T(t), E(t), I(t) and F(t).

$$\frac{dH}{dt} = H\left[g_1 - d_1 H - kT\right] - c_1 HE, \tag{1}$$

$$\frac{dT}{dt} = T\left[g_2 - d_2 T - z_1 I\right] + c_2 HE + m_3 TF, \tag{2}$$

$$\frac{dI}{dt} = s + I\left[\frac{\phi T}{\omega_1 + T} - \frac{c_3 E}{\omega_2 + E} - \mu - z_2 T\right], \tag{3}$$

$$\frac{dE}{dt} = \theta_1 - \theta_2 E + m_2 FE, \tag{4}$$

$$\frac{dF}{dt} = g_3 F\left(1 - m_1 F\right). \tag{5}$$

3. MATHEMATICAL REPRESENTATION

Mathematical representation of five-dimensional ODE's by putting the values of parameters is as follows:

Case 1

$$\begin{aligned}
\frac{dH}{dt} &= H\left[0.65 - 0.30H - 1T\right] - 0.15HE,\\
\frac{dT}{dt} &= T\left[0.98 - 0.40T - 1I\right] + 0.7HE + 0.5TF,\\
\frac{dT}{dt} &= 0.4 + I\left[\frac{0.8T}{0.9+T} - \frac{0.07E}{0.1+E} - 0.1 - 0.5T\right],\\
\frac{dT}{dt} &= 0.9 - 0.8788E + 0.2562FE\\
\frac{dT}{dt} &= 0.30F(1 - 0.5F)
\end{aligned} \tag{6}$$

Case 2

$$\begin{aligned}
\frac{dH}{dt} &= H\left[0.70 - 0.30H - 1T\right] - 0.15HE,\\
\frac{dT}{dt} &= T\left[0.98 - 0.40T - 1I\right] + 0.5HE + 0.5TF,\\
\frac{dT}{dt} &= 0.4 + I\left[\frac{0.8T}{0.9+T} - \frac{0.06E}{0.1+E} - 0.1 - 0.5T\right],\\
\frac{dT}{dt} &= 0.9 - 0.8788E + 0.2562FE\\
\frac{dT}{dt} &= 0.30F(1 - 0.6F)
\end{aligned} \tag{7}$$

Case 3

$$\begin{aligned}
\frac{dH}{dt} &= H\left[0.75 - 0.30H - 1T\right] - 0.15HE,\\
\frac{dT}{dt} &= T\left[0.98 - 0.40T - 1I\right] + 0.4HE + 0.5TF,\\
\frac{dT}{dt} &= 0.4 + I\left[\frac{0.8T}{0.9+T} - \frac{0.09E}{0.1+E} - 0.1 - 0.5T\right],\\
\frac{dT}{dt} &= 0.9 - 0.8788E + 0.2562FE\\
\frac{dT}{dt} &= 0.30F(1 - 0.8F)
\end{aligned} \tag{8}$$

Case 4

$$\frac{dH}{dt} = H\left[0.73 - 0.30H - 1T\right] - 0.15HE,$$

$$\frac{dT}{dt} = T\left[0.98 - 0.40T - 1I\right] + 0.6HE + 0.5TF,$$

$$\frac{dT}{dt} = 0.4 + I\left[\frac{0.8T}{0.9+T} - \frac{0.10E}{0.1+E} - 0.1 - 0.5T\right], \quad (9)$$

$$\frac{dT}{dt} = 0.9 - 0.8788E + 0.2562FE$$

$$\frac{dT}{dt} = 0.30F(1 - 0.9F)$$

4. SOLUTION METHODOLOGY

This section describes the solution methodology of ordinary differential equations (ODE's) equations 1 to 5 for breast cancer risk model. Synthetic dataset is generated by applying Adams numerical method, BDF method, explicit Runge Kutta and implicit Runge Kutta method using Mathematica ND-solve in Mathematica software. The data set is generated for four scenarios, each having four cases with step size of 0.2. The variations of different parameters for breast cancer risk models are shown in Table 1.

Table 1 Scenarios and cases of risk breast cancer

Scenario-1: *g1*	Scenario-2: *c2*	Scenario-3:	Scenario-4: m1
Case 1: 0.65	Case 1: 0.7	Case 1: 0.07	Case 1: 0.5
Case 2: 0.70	Case 2: 0.5	Case 2: 0.06	Case 2: 0.6
Case 4: 0.75	Case 4: 0.4	Case 4: 0.09	Case 4: 0.8
Case 5: 0.73	Case 5: 0.6	Case 5: 0.10	Case 5: 0.9

. RESULTS AND DISCUSSION

In this section mathematical modeling for breast cancer risk model BCRM is articulated by comparing outcomes produced by Adams' numerical method, BDF method, explicit Runge-kutta method and implicit Runge-kutta method. By using solution graphs and absolute error plots for proposed BCRM breast cancer risk model shows connection between certain parameters like healthy breast cells logistic-growth rate (g1), rate of overflowing estrogen from DNA (c2), rate of immune suppression rate with estrogen (c3) and fat carrying capacity rate (m1). In Mathematica software for breast cancer risk model BCRM the synthetic dataset is generated numerically with the help of ND solver by using four techniques i.e. Adams' numerical approach, BDF, implicit Runge-kutta technique and implicit Runge-kutta technique. The data set is created for four scenarios each having four cases, putting t (0,100) with step size of 0.2. The generated synthetic dataset is then relocated to MATLAB to analyze the difference between BDF technique and Adams' numerical method for g1 (logistic growth rate of healthy breast cells) and c2 (rate of overflowing estrogen from DNA, also analyzed the comparison between c3 (rate of immune suppression by estrogen) and m1 (inverse rate of fat carrying capacity) through explicit Runge-kutta method and implicit Runge-kutta technique. Solution graph plots and absolute error plots depicted the proficiency for BCRM. The solution plots of breast cancer risk model for healthy cells, tumor cells, immune cells, estrogen and fat cells portrays in figure (2-5) and subfigures 2 (i, ii, iii, iv, v) – 5 (i, ii, iii, iv, v). In figure 2 and subfigures 2(i, ii, iii, iv, v) by varying parameter g1= 0.65, 0.70, 0.75, 0.73 representing logistic growth rate of healthy breast cells initially decreased then increased and eventually stabilized at a constant value to the healthy cells H(t). In all four scenarios, the values of tumor cells T(t) decreased and then stabilized at a constant rate against time. The values of immune cells I(t) increased over time. Estrogen level E(t) initially decreased, then increased and finally with the increase in time. Fat cells F(t) increased initially and then stabilized as time progressed. Approximately the same results found in figure 3 and subfigures 3(i, ii, iii, iv, v) for all five variables i.e. healthy cells, tumor cells, immune cells, estrogen level and fat cells while comparing the results of Adams' and BDF with analyses on Solution graphs for breast cancer risk model for Scenario 2 of four cases by varying parameter c2= 0.7, 0.5, 0.4, 0.6 representing rate of overflowing estrogen from DNA. In figure 4 and subfigures 4(i, ii, iii, iv, v) by varying values of parameter c3= 0.07, 0.06, 0.09, 0.10 rate of immune suppression by estrogen in four cases of scenario 3 by comparing results of explicit Runge-kutta and explicit Runge-kutta, initially decreased, then increased and eventually stabilized in H(t). values of T(t) initially declined and then stabilized at a constant rate, whereas the values of I(t) consistently rose over time, indicating an adaptive response. E(t) first decreased then increased and finally stabilized as time progressed, similarly F(t) showed an initial increase before reaching a steady state over time. Figure 5 and subfigures 5(i, ii, iii, iv, v) showed comparison of results of explicit and implicit Runge-kutta by varying parameter m1=0.5, 0.6, 0.8, 0.9 inverse rate of fat carrying capacity. The solution graphs of estrogen level and fat cells showed the same pattern but with much more variations. The remaining graphs showed the same pattern as observed with earlier techniques.

Figure 6 and subfigures 6(i, ii, iii, iv, v) showed comparative view of healthy cells H(t), tumor cells T(t), immune cells I(t), estrogen level E(t) and fat cells F(t) under four different cases over time, different curves labeled AE-C1, AE C-2, AE C-4 and AE C-5. The x-axis represented time ranging from 0 to 100, y-axis representing logarithmic scale, values from 10^{-5} to 10^{-11} for healthy cells suggest that the values of H(t) cover a broad range with some curves dipping in to very small values, whereas the values from 10^{-5} to 10^{-10} for all other curves including tumor, immune, estrogen and fat cells. All curves follow a downward trend with fluctuations at various points, indicating gradual decrease in cell counts with some variability in measurement. The variability and patterns in the progression of cells shown in the graphs, logarithmic scale visualized changes across a wide range from minor fluctuations to more significant peaks and dips. Figure 7 and subfigure 7(i, ii, iii, iv, v) showed comparison of the results of Adams' and BDF with analyses on absolute error graphs for breast cancer risk model for scenario 2 of four cases by varying parameter c2= 0.7, 0.5, 0.4, 0.6 along with values on y-axis ranging from lowest value 10^{-4} to highest value 10^{-10} for H(t), T(t), I(t), E(t) and F(t) depicting progression of cells in graphs. The graphs in figure 8-9 and subfigure 8-9(i, ii, iii, iv, v) depict results of explicit Runge-kutta and implicit Runge-kutta along values on y-axis ranging from 10-0 to 10-16 from lowest to highest with analyses on absolute error graphs for breast cancer risk model for scenario 3 of four cases by varying parameter c3= 0.07, 0.06, 0.09, 0.10 (for figure 8) m1= 0.5, 0.6, 0.8, 0.9 (for figure 9). AE C-1 shows downward trends with some

fluctuations, rapid increase and then dips again near the end. AE C-2 and AE C-4 display similar fluctuating behavior with some overlapping points.AE C-5 remains relatively stable and high on the graph indicating higher values than the other datasets.

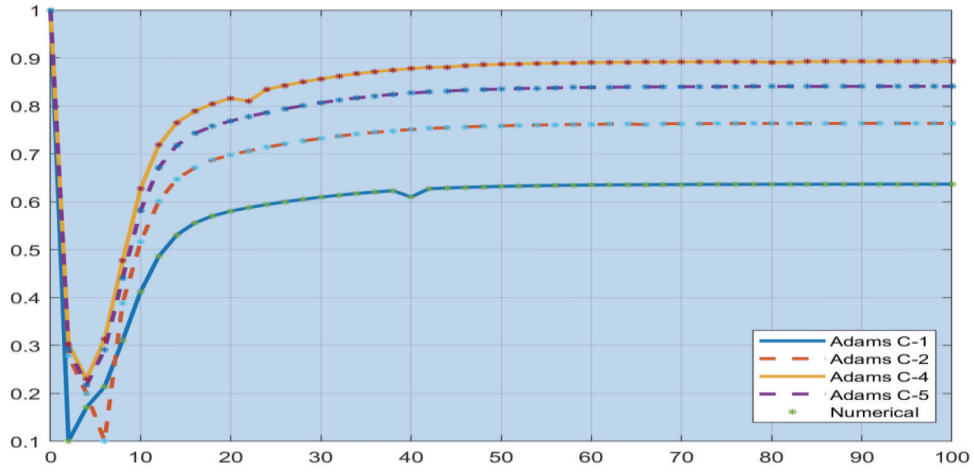

2 (i) Solution graph outcomes for H(t)

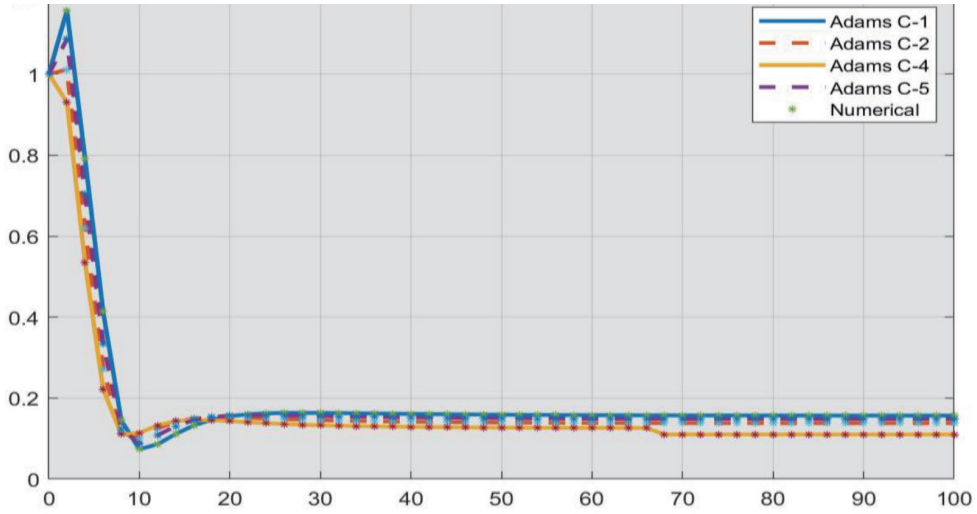

2 (ii) Solution graph outcomes for T(t)

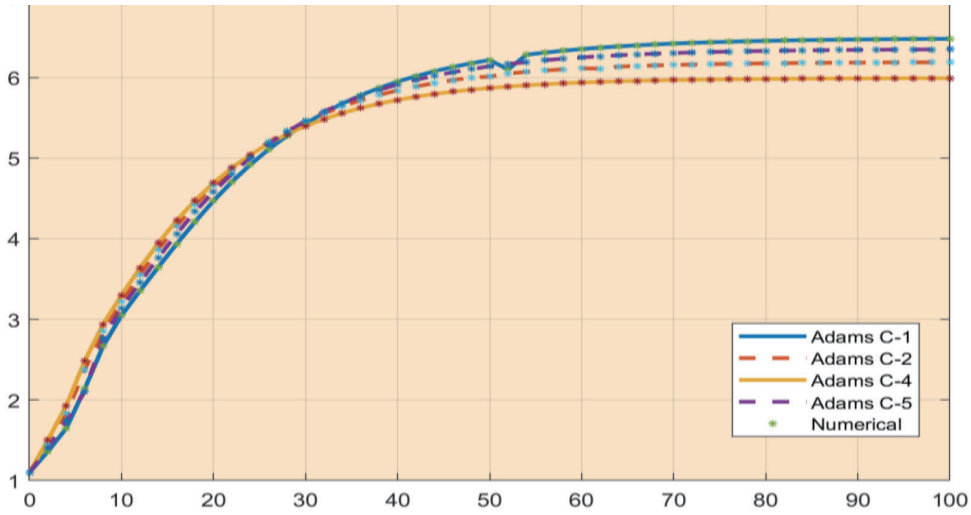

2 (iii) Solution grap outcomes for I(t)

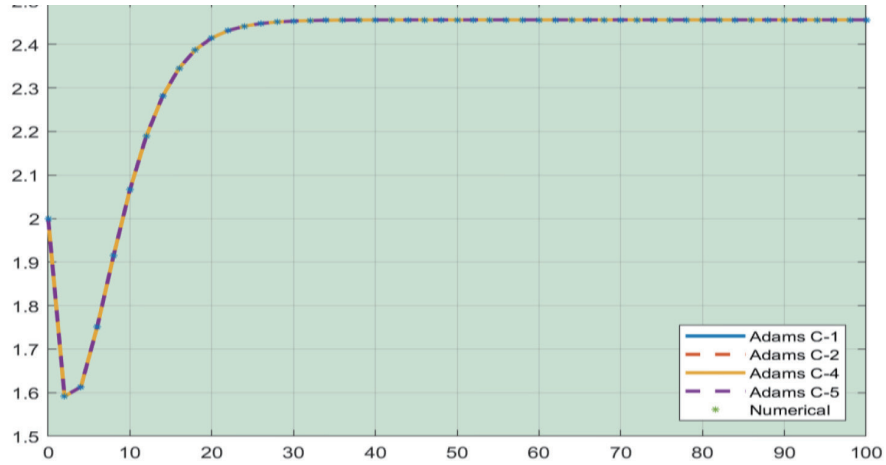

2 (iv) Solution graph outcomes for E(t)

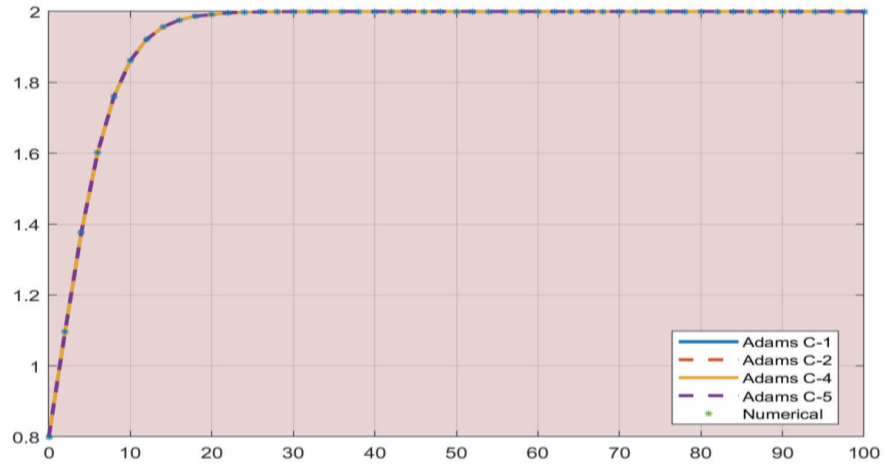

2 (v) Solution graph outcomes for F(t)

Fig. 2 Comparison of the results of Adams' and BDF with analyses on Solution graphs for BCR model for Scenario 1 of four cases by varying parameter g1= 0.65, 0.75, 0.73.

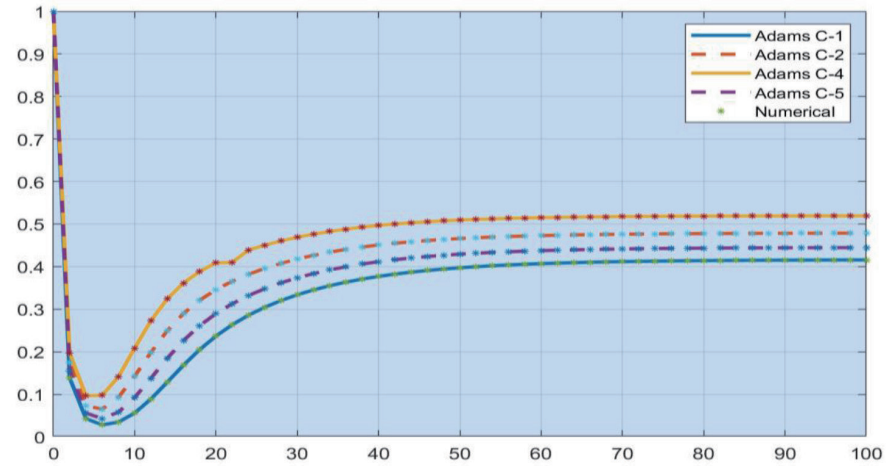

3 (i) Solution graph outcomes for H(t)

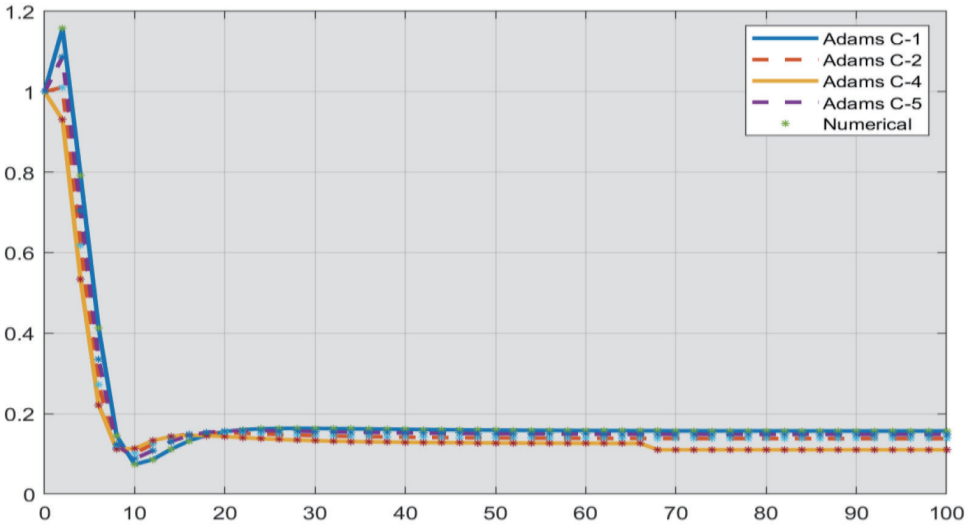

3 (ii) Solution graph outcomes for T(t)

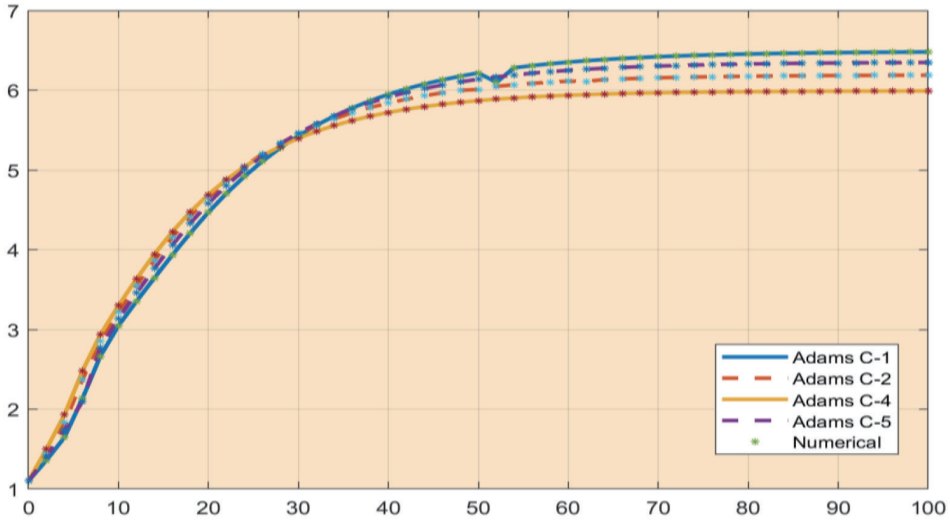

3 (iii) Solution graph outcomes for I(t)

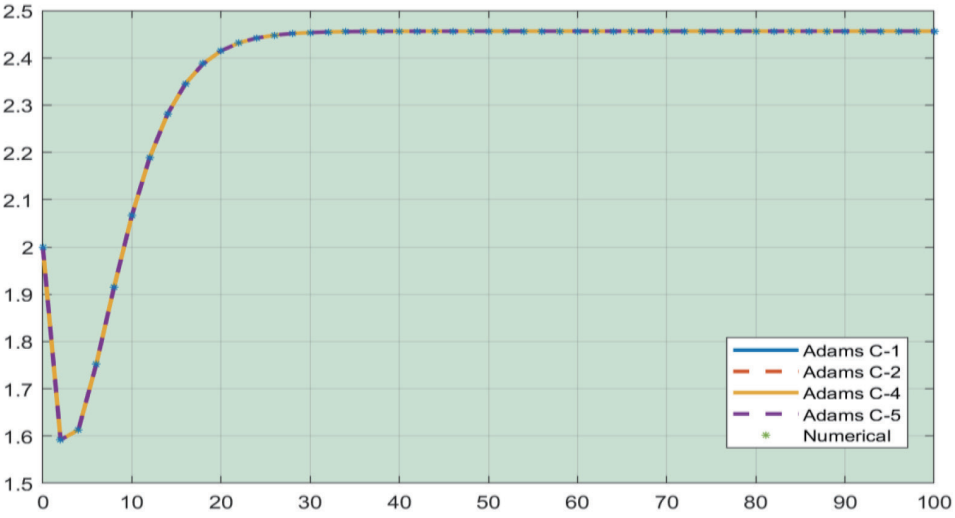

3 (iv) Solution graph outcomes for E(t)

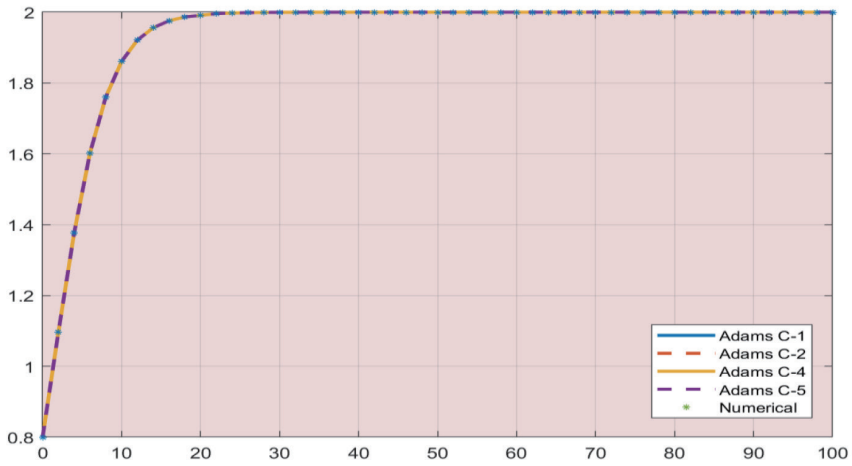

3 (v) Solution graph outcomes for F(t)

Fig. 3 Comparison of the results of Adams' and BDF with analyses on Solution graphs for BCR model for Scenario 2 of four cases by varying parameter c2= 0.7, 0.5, 0.4, 0.6.

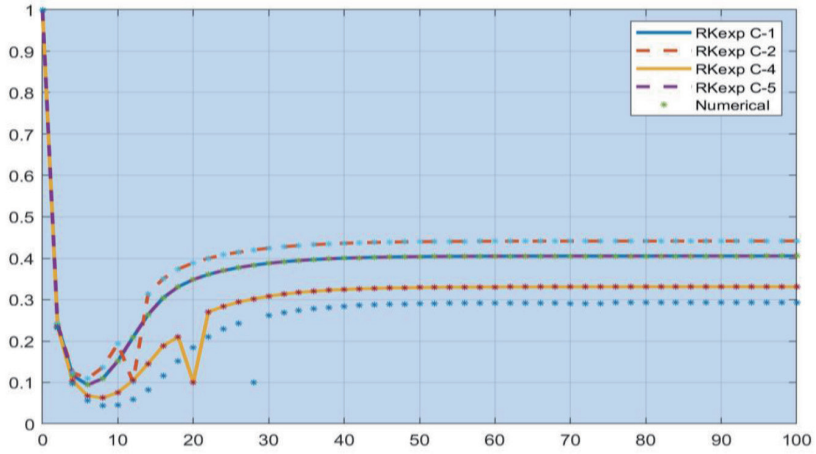

4 (i) Solution graph outcomes for H(t)

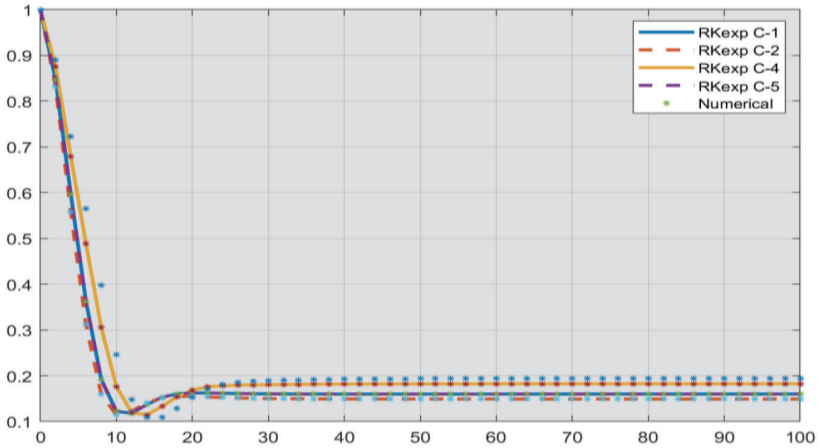

4 (ii) Solution graph outcomes for T(t)

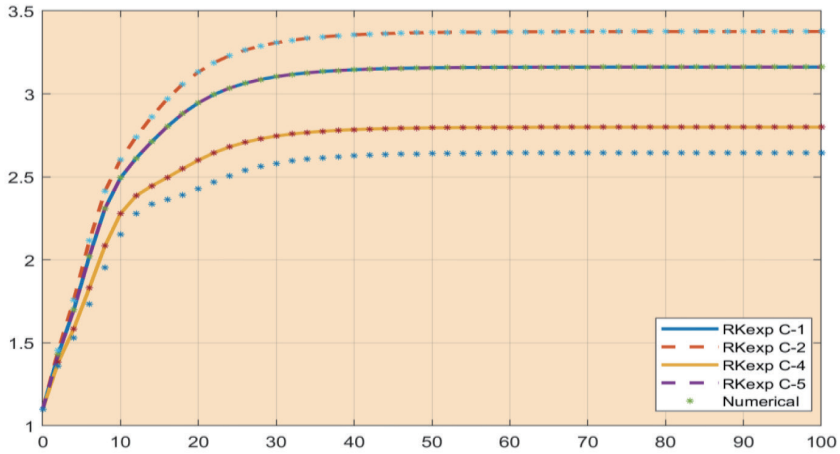

4 (iii) Solution graph outcomes for I(t)

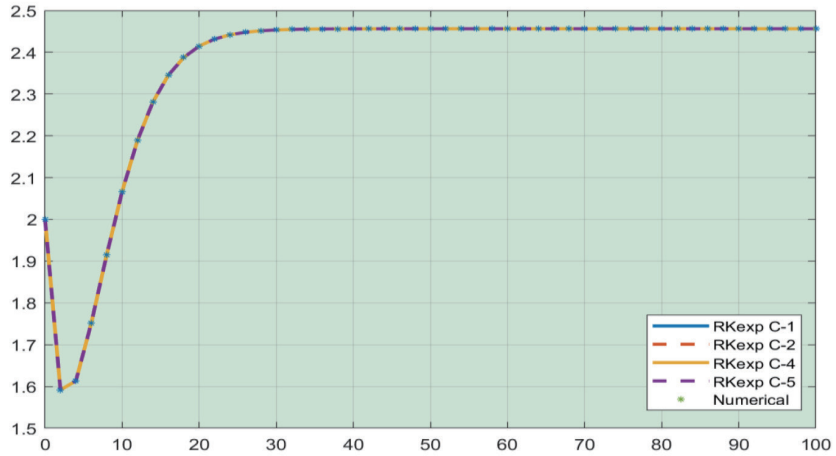

4 (iv) Solution graph outcomes for E(t)

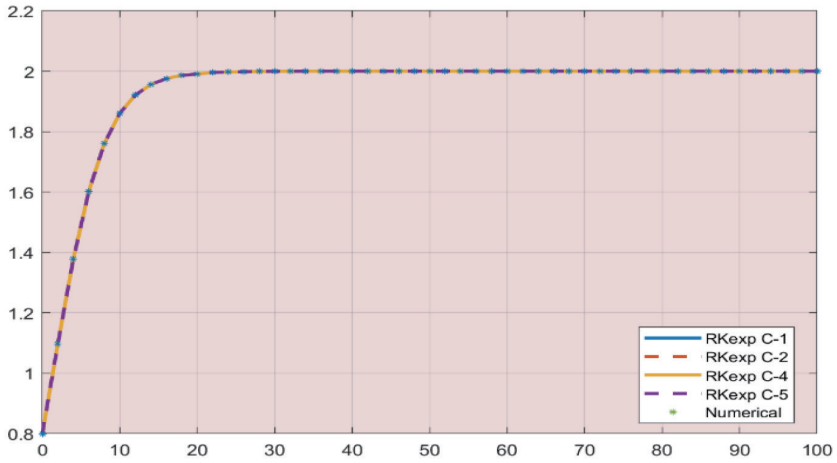

4 (v) Solution graph outcomes for F(t)

Fig. 4 Comparison of the results of explicit Runge-kutta and implicit Runge-kutta with analyses on Solution graphs for BCR model for Scenario 3 of four cases by varying parameter c3= 0.07, 0.06, 0.09, 0.10.

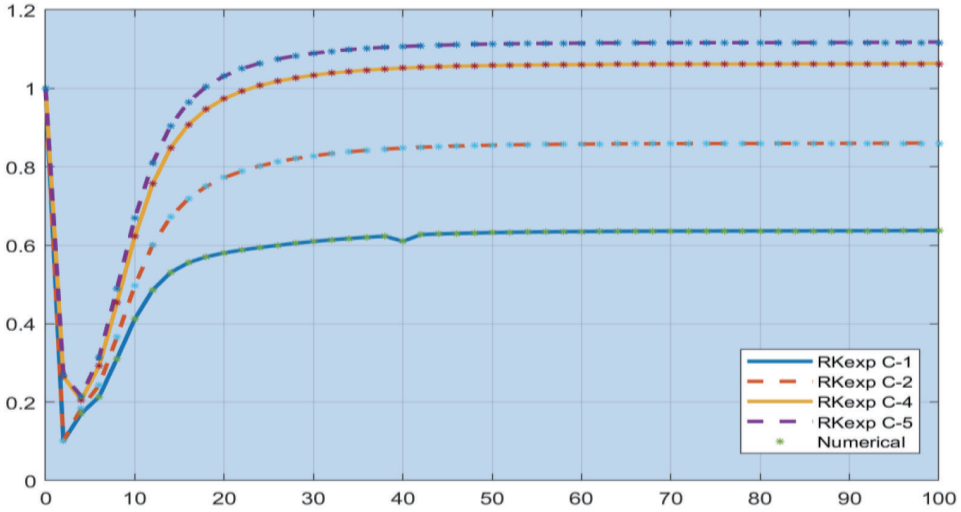

5 (i) Solution graph outcomes for H(t)

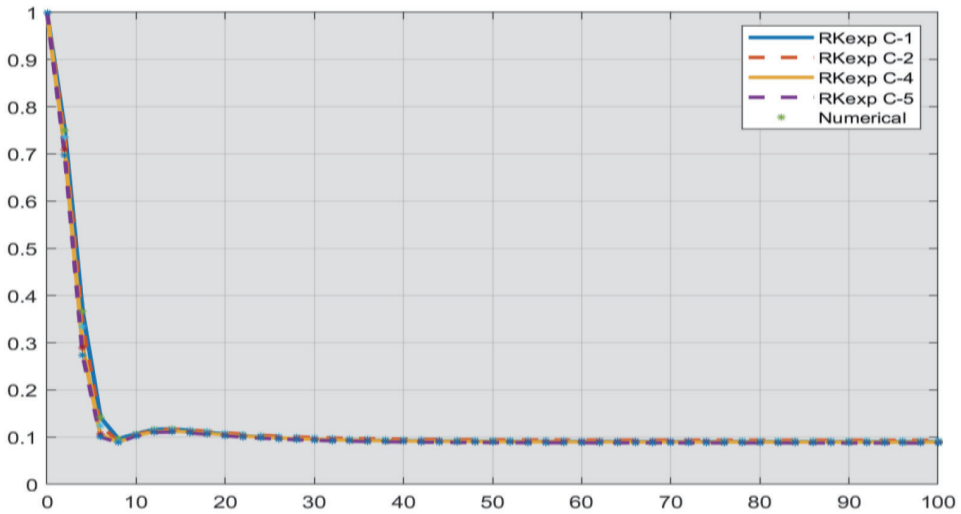

5 (ii) Solution graph outcomes for T(t)

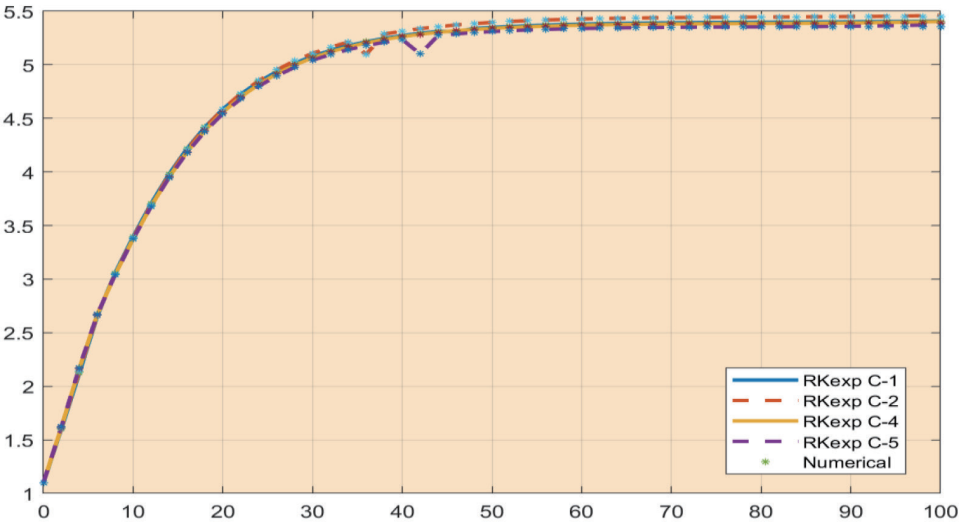

5 (iii) Solution graph outcomes for I(t)

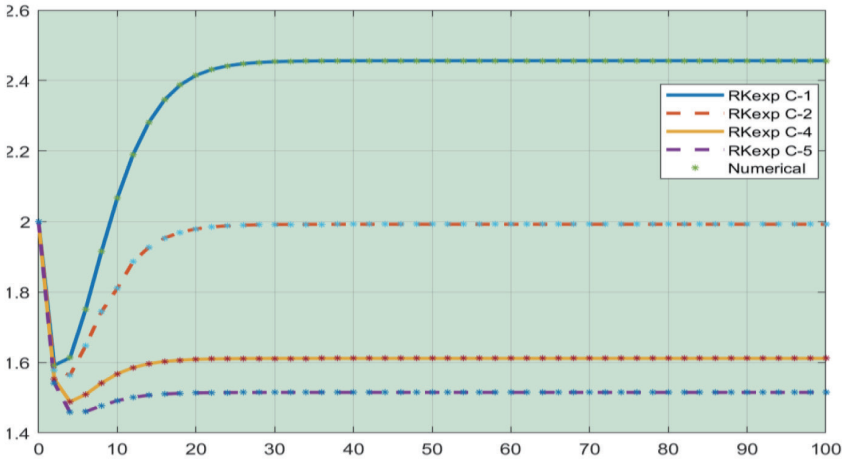

5 (iv) Solution graph outcomes for E(t)

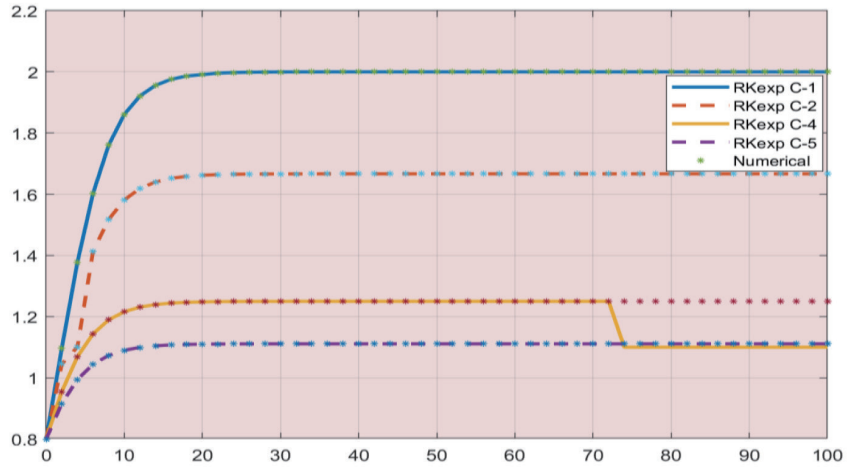

5 (v) Solution graph outcomes for F(t)

Fig. 5 Comparison of the results of explicit Runge-kutta and implicit Runge-kutta with analyses on Solution graphs for BCR model for Scenario 4 of four cases by varying parameter m1= 0.5, 0.6, 0.8, 0.9.

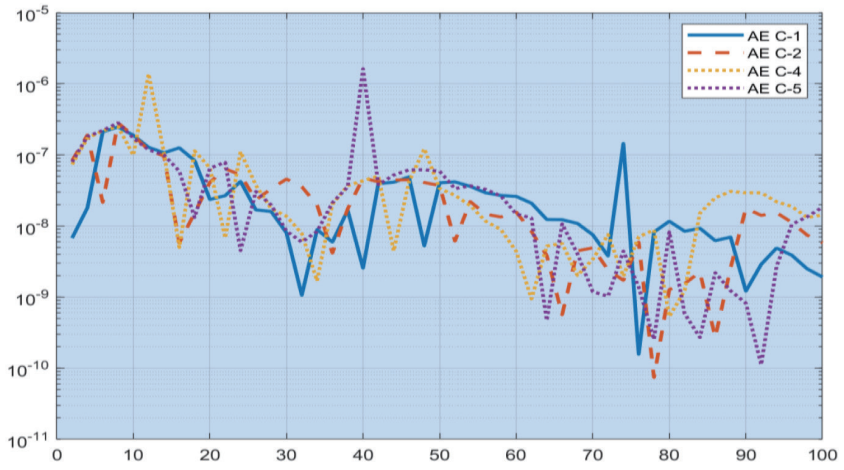

6 (i) Absolute Error graph outcomes for H(t)

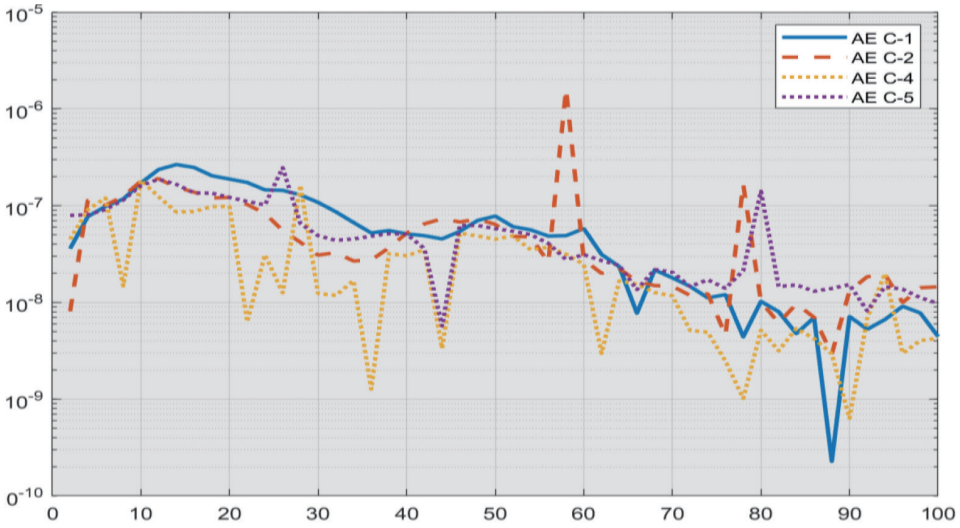

6 (ii) Absolute Error graph outcomes for T(t)

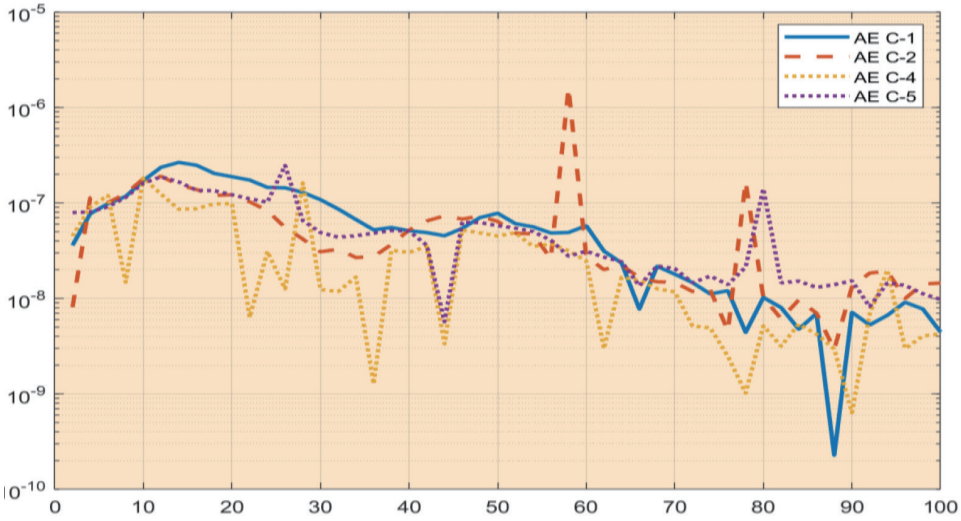

6 (iii) Absolute Error graph outcomes for I(t)

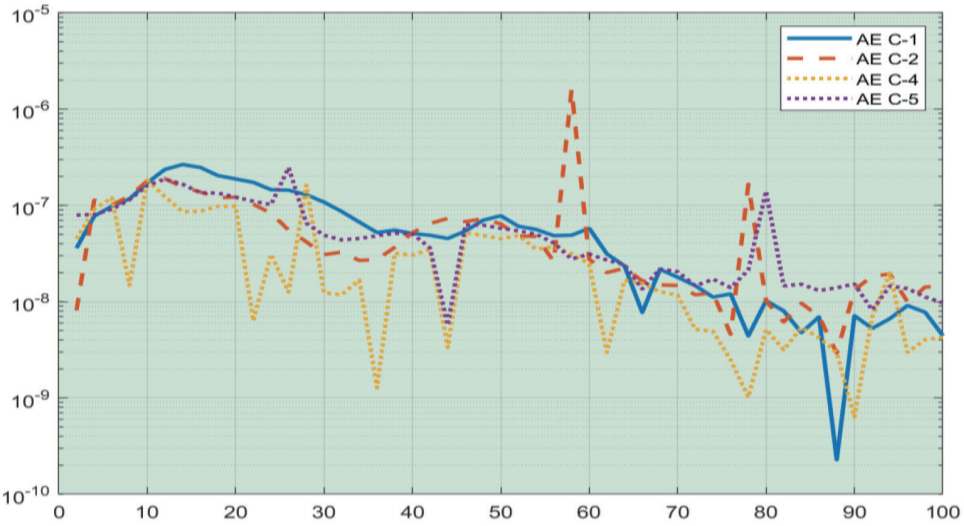

6 (iv) Absolute Error graph outcomes for E(t)

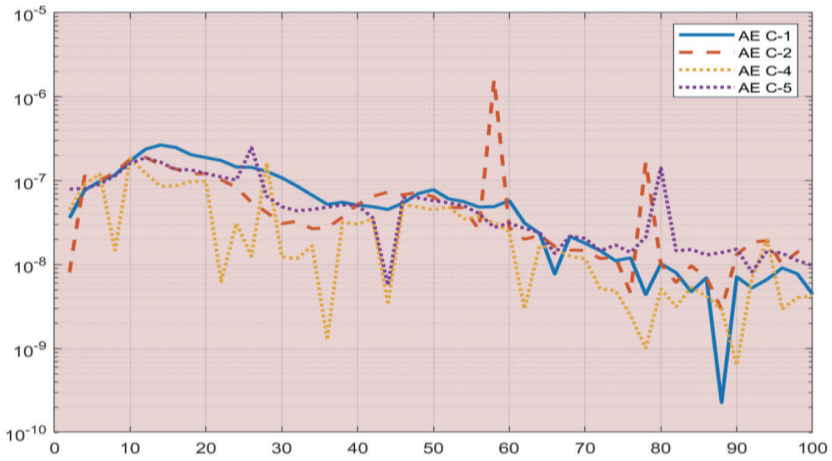

6 (v) Absolute Error graph outcomes for F(t)

Fig. 6 Comparison of the results of Adams' and BDF with analyses on Absolute Error graphs for BCR model for Scenario 1 of four cases by varying parameter g1= 0.65, 0.70, 0.75, 0.73.

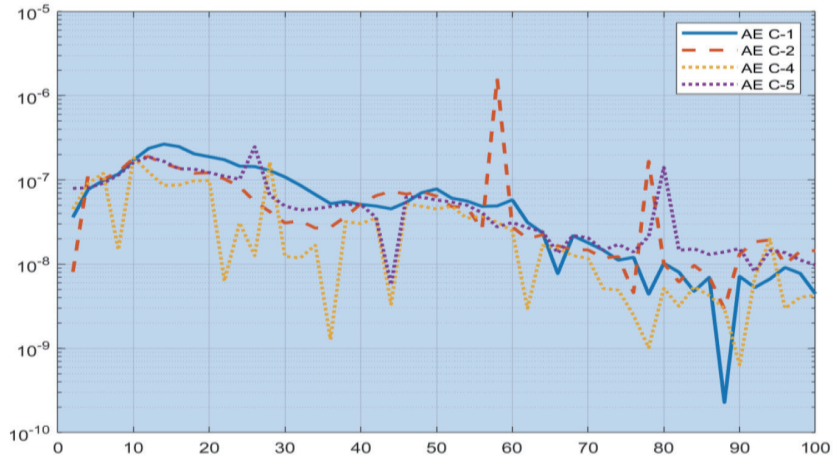

7 (i) Absolute Error graph outcomes for H(t)

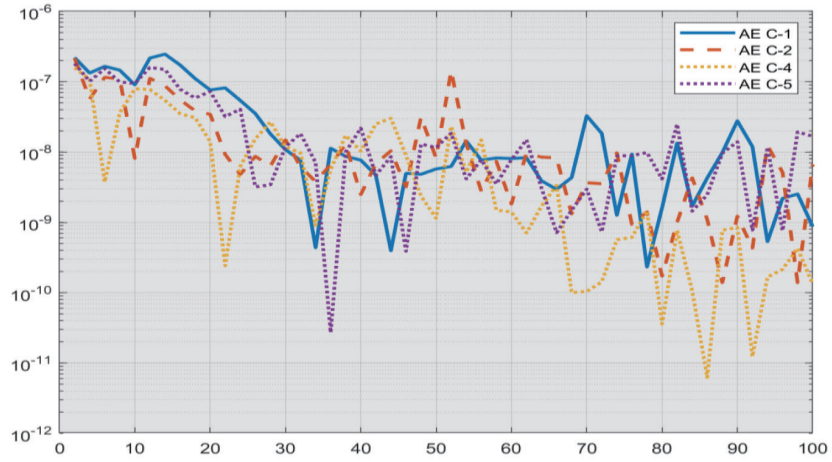

7 (ii) Absolute Error graph outcomes for T(t)

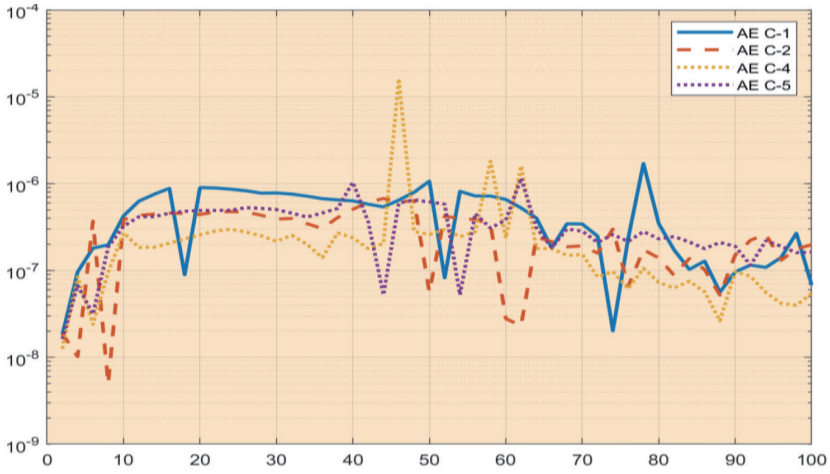

7 (iii) Absolute Error graph outcomes for I(t)

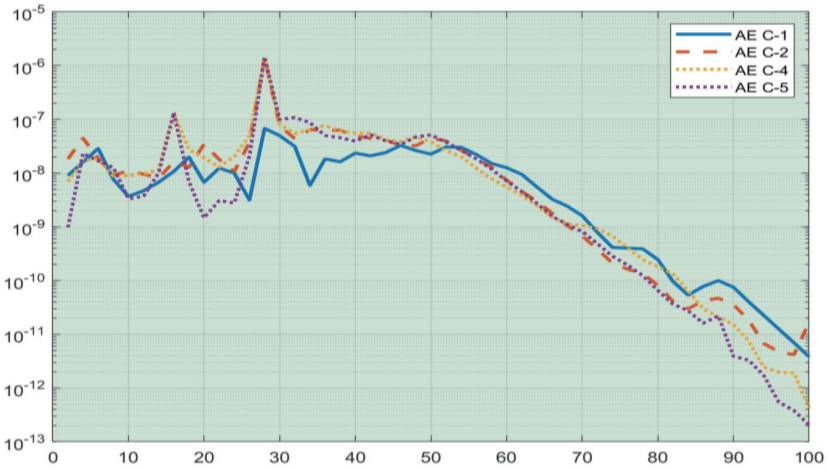

7 (iv) Absolute Error graph outcomes for E(t)

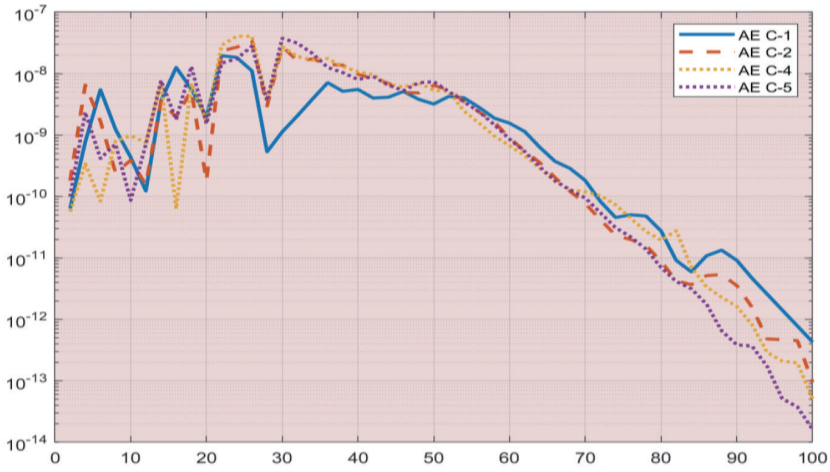

7 (v) Absolute Error graph outcomes for F(t)

Fig. 7 Comparison of the results of Adams' and BDF with analyses on Absolute Error graphs for BCR model for Scenario 2 of four cases by varying parameter c2= 0.7, 0.5, 0.4, 0.6.

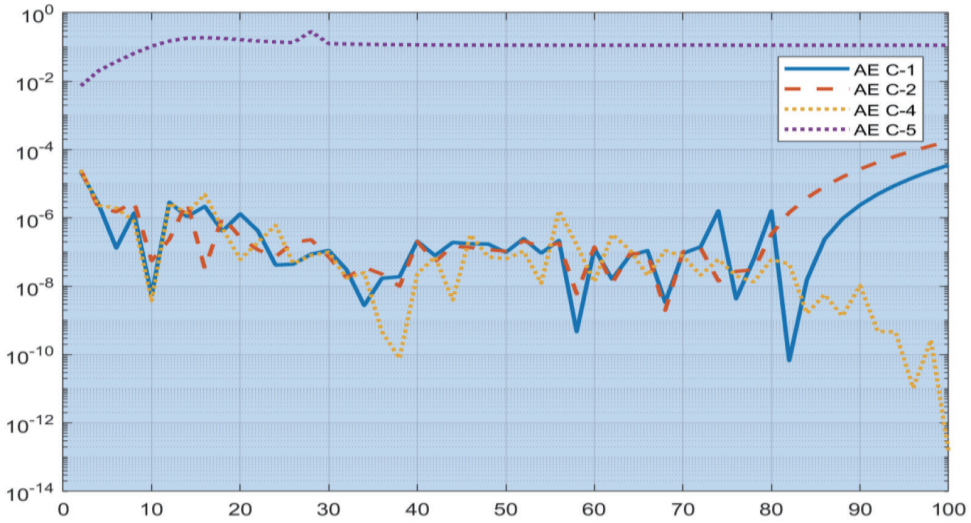

8 (i) Absolute Error graph outcomes for H(t)

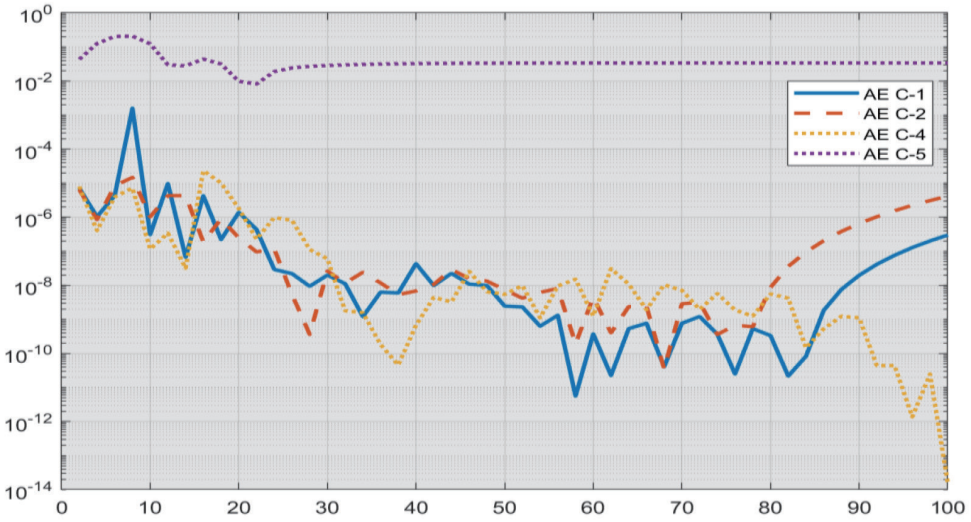

8 (ii) Absolute Error graph outcomes for T(t)

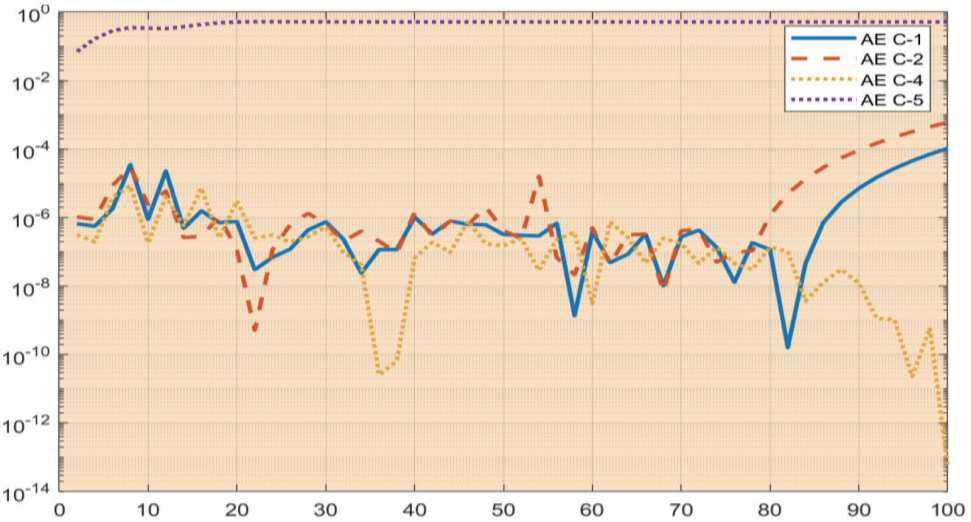

8 (iii) Absolute Error graph outcomes for I(t)

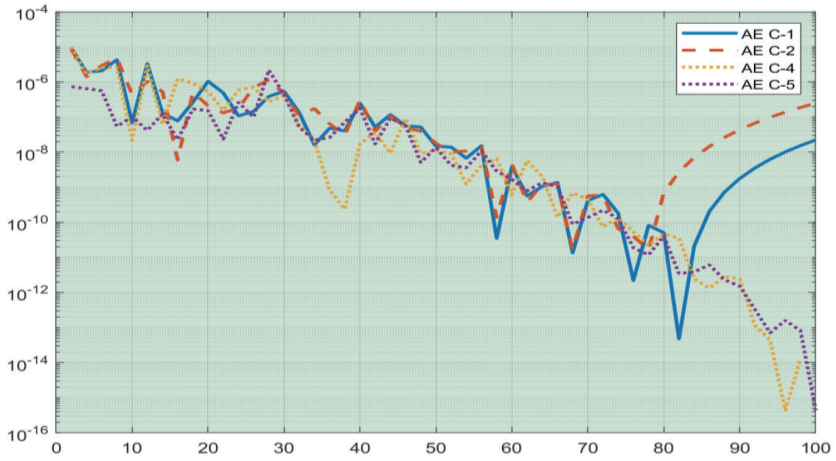

8 (iv) Absolute Error graph outcomes for E(t)

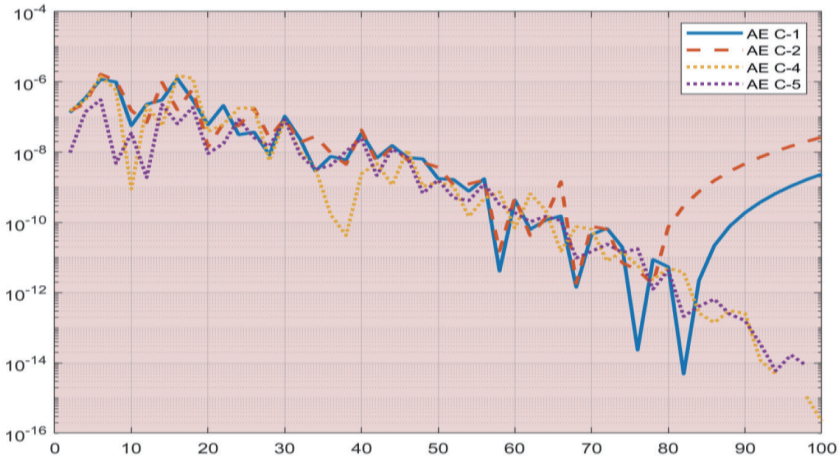

8 (v) Absolute Error graph outcomes for F(t)

Fig. 8 Comparison of the results of explicit Runge-kutta and implicit Runge-kutta with analyses on Absolute Error graphs for BCR model for Scenario 3 of four cases by varying parameter c3= 0.07, 0.06, 0.09, 0.10.

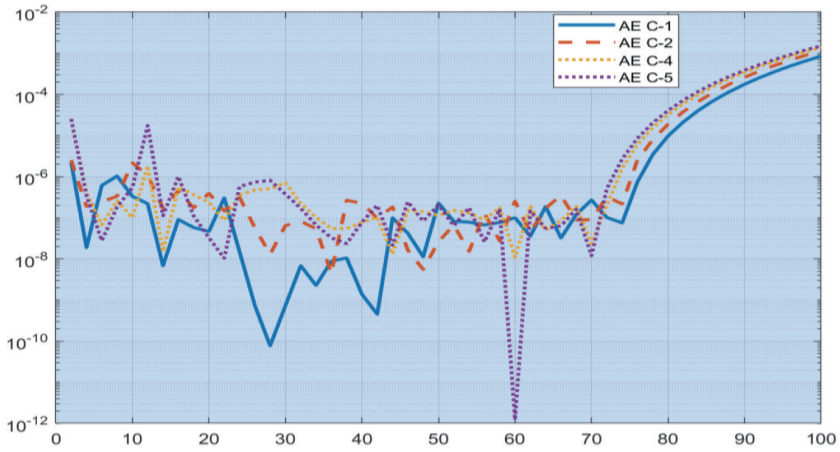

9 (i) Absolute Error graph outcomes for H(t)

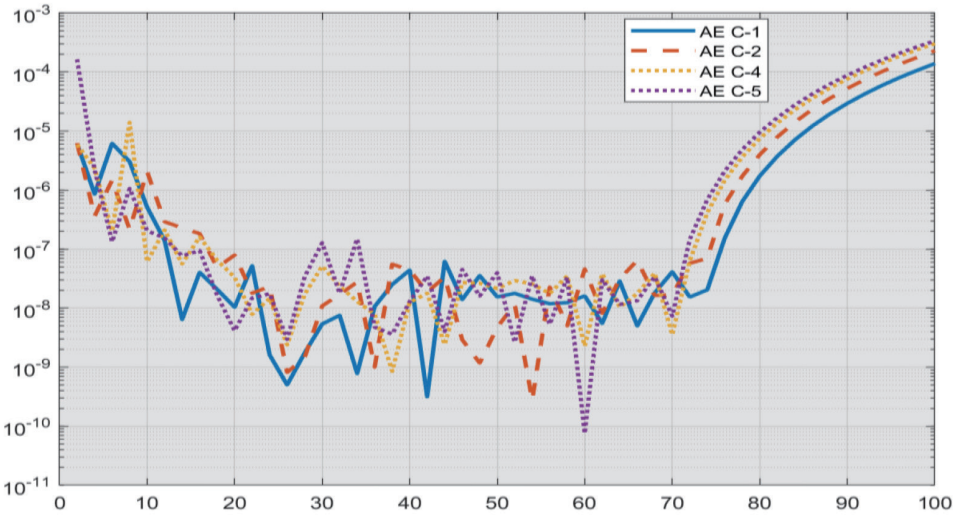

9 (ii) Absolute Error graph outcomes for T(t)

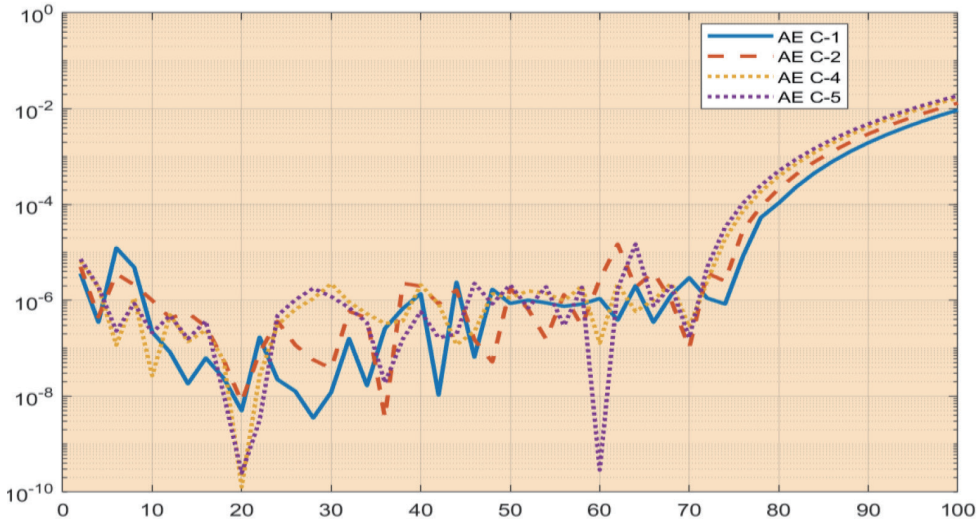

9 (iii) Absolute Error graph outcomes for I(t)

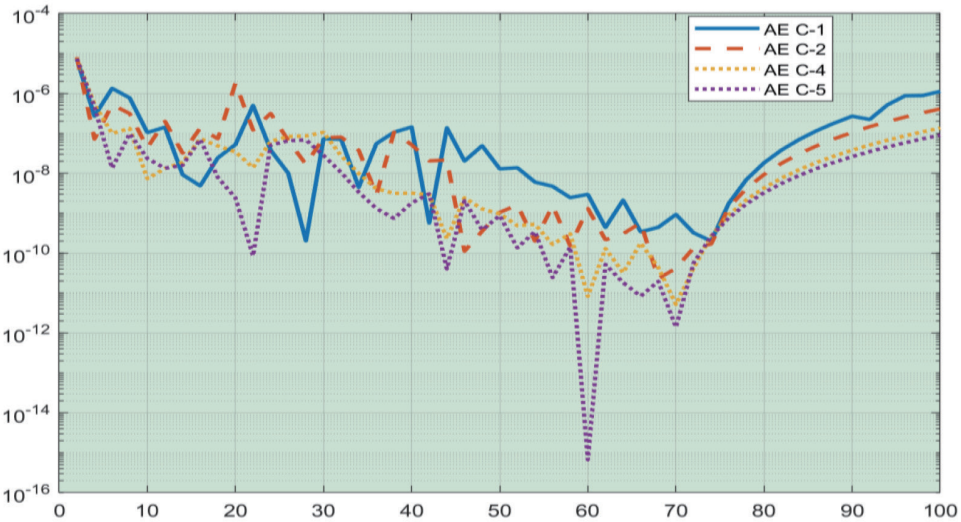

9 (iv) Absolute Error graph outcomes for E(t)

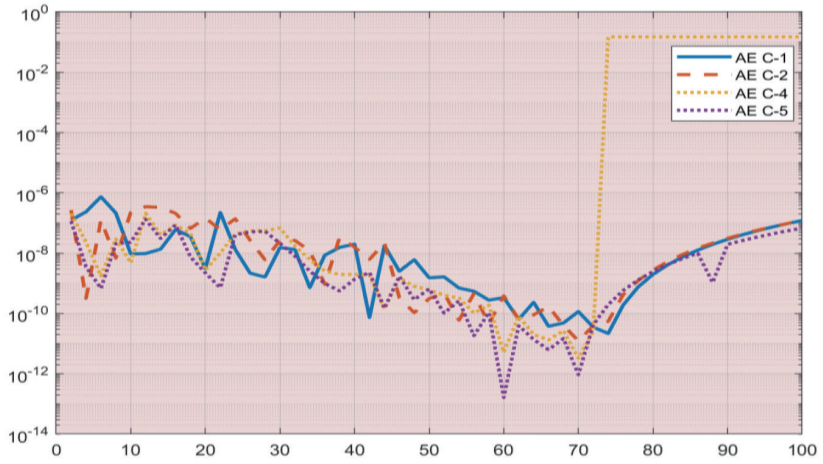

9 (v) Absolute Error graph outcomes for F(t)

Fig. 9 Comparison of the results of explicit Runge-kutta and implicit Runge-kutta with analyses on Absolute Error graphs for BCR model for Scenario 4 of four cases by varying parameter m1= 0.5, 0.6, 0.8, 0.9.

6. CONCLUSION

This study demonstrates the effectiveness of various numerical methods i.e. Adams' numerical solver, BDF method, explicit Runge-kutta method and implicit Runge-kutta technique in approximating solutions for breast cancer risk model through ordinary differential equations (ODE's). The synthetic dataset created through ND-solve, with parameters l healthy breast cells logistic-growth rate, rate of overflowing estrogen from DNA, rate of immune suppression rate with estrogen and fat carrying capacity rate adjustments to simulate biological factors influencing breast cancer risk, enabled comparative analysis across methods. Further absolute error plots and solution plots reveal these methods' relative accuracy and computational robustness. For precise and reliable breast cancer risk assessment, the findings underscore the potential of integrating advanced numerical techniques-based solutions paving the way for more effective predictive modeling in oncology. This ODE-based framework has the potential to serve as a foundational tool for researchers and clinicians, offering insight into the temporal aspects of cancer risk and supporting interventions that target modifiable risk factors related to body composition.

REFERENCES

[1] Chermon, D. and Birk, R., 2024. "Deciphering the Interplay between Genetic Risk Scores and Lifestyle Factors on Individual Obesity Predisposition." *Nutrients,* **16**(9), p.1296.

[2] Bray, F., Laversanne, M., Sung, H., Ferlay, J., Siegel, R.L., Soerjomataram, I. and Jemal, A., 2024. "Global cancer statistics 2022: GLOBOCAN estimates of incidence and mortality worldwide for 36 cancers in 185 countries." *CA: a cancer journal for clinicians*, **74**(3), pp.229-263.

[3] Bizuayehu, H.M., Dadi, A.F., Hassen, T.A., Ketema, D.B., Ahmed, K.Y., Kassa, Z.Y., Amsalu, E., Kibret, G.D., Alemu, A.A., Alebel, A. and Shifa, J.E., 2024. "Global burden of 34 cancers among women in 2020 and projections to 2040: Population-based data from 185 countries/territories." *International journal of cancer,* **154**(8), pp.1377-1393.

[4] Dumitrescu, R.G. and Cotarla, I.J.J.O.C., 2005. "Understanding breast cancer risk-where do we stand in 2005?." *Journal of cellular and molecular medicine,* **9**(1), pp.208-221.

[5] Johariya, V., Joshi, A., Malviya, N. and Malviya, S., 2024. "Introduction to Cancer." *In Medicinal Plants and Cancer Chemoprevention* (pp. 1-28). CRC Press.

[6] Stanger, B.Z. and Wahl, G.M., 2024. "Cancer as a Disease of Development Gone Awry." *Annual Review of Pathology: Mechanisms of Disease,* **19**(1), pp.397-421.

[7] Subedi, R., Houssami, N., Nickson, C., Nepal, A., Campbell, D., David, M. and Yu, X.Q., 2024. "Factors influencing the time to diagnosis and treatment of breast cancer among women in low- and middle-income countries: A systematic review*." The Breast,* p.103714.

[8] Bray, F., Laversanne, M., Sung, H., Ferlay, J., Siegel, R.L., Soerjomataram, I. and Jemal, A., 2024."Global cancer statistics 2022: GLOBOCAN estimates of incidence and mortality worldwide for 36 cancers in 185 countries." *CA: a cancer journal for clinicians,* **74**(3), pp.229-263.

[9] Cuthrell, K.M. and Tzenios, N., 2023. "Breast Cancer: Updated and Deep Insights." *International Research Journal of Oncology,* **6**(1), pp.104-118.

[10] Abd-Elsalam Sheleg, E.M., 2024. *Biology of risk factors in the origination of breast cancer and their role in early detection* (Doctoral dissertation, جامعة الزاوية-university of zawia).

[11] Javed, MU, Javaid, N., Alrajeh, N., Shafiq, M., & Choi, JG (2024). "Mutual authentication enabled trust model for vehicular energy networks using Blockchain in Smart Healthcare Systems." *Simulation Modelling Practice and Theory,* **136** , 103006.

[12] Jaffe, E.S., Harris, N.L., Stein, H. and Isaacson, P.G., 2008. "Classification of lymphoid neoplasms: the microscope as a tool for disease discovery. *Blood,* **112**(12), pp.4384-4399.

[13] Finn, R.S., Press, M.F., Dering, J., Arbushites, M., Koehler, M., Oliva, C., Williams, L.S. and Di Leo, A., 2009. "Estrogen receptor, progesterone receptor, human epidermal growth factor receptor 2 (HER2), and epidermal growth factor receptor expression and benefit from lapatinib in a randomized trial of paclitaxel with lapatinib or placebo as first-line treatment in HER2-negative or unknown metastatic breast cancer." *Journal of clinical oncology,* **27**(24), pp.3908-3915.

[14] Nounou, M.I., ElAmrawy, F., Ahmed, N., Abdelraouf, K., Goda, S. and Syed-Sha-Qhattal, H., 2015. "Breast cancer: conventional diagnosis and treatment modalities and recent patents and technologies." *Breast cancer: basic and clinical research*, **9**, pp.BCBCR-S29420.)

[15] Van Goethem, M., Tjalma, W., Schelfout, K., Verslegers, I., Biltjes, I. and Parizel, P., 2006. "Magnetic resonance imaging in breast cancer." *European Journal of Surgical Oncology (EJSO),* **32**(9), pp.901-910.

[16] Moser, E., Stadlbauer, A., Windischberger, C., Quick, H.H. and Ladd, M.E., 2009. "Magnetic resonance imaging methodology." *European journal of nuclear medicine and molecular imaging,* **36**, pp.30-41.

[17] Ruiter, N.V., Stotzka, R., Muller, T.O., Gemmeke, H., Reichenbach, J.R. and Kaiser, W.A., 2006. "Model-based registration of X-ray mammograms and MR images of the female breast." *IEEE transactions on nuclear science,* **53**(1), pp.204-211.

[18] Brettle, D.S., Ward, S.C., Parkin, G.J.S., Cowen, A.R. and Sumsion, H.J., 1994. "A clinical comparison between conventional and digital mammography utilizing computed radiography." *The British Journal of Radiology,* **67**(797), pp.464-468.

[19] Guo, S., Han, L. and Guo, Y., Advanced Technologies in Healthcare.

[20] Mele, C., De Marchi, L., Marsan, G., Zavattaro, M., Mauri, M.G., Aluffi Valletti, P., Aimaretti, G. and Marzullo, P., 2024. "The Role of Body Mass Index (BMI) in Differentiated Thyroid Cancer: A Potential Prognostic Factor?." *Biomedicines,* **12**(9), p.1962.

[21] Quartuccio, N., Ialuna, S., Pulizzi, S., D'Oppido, D., Antoni, M. and Moreci, A.M., 2024. "The Correlation of Body Mass Index with Risk of Recurrence in Post-Menopausal Women with Breast Cancer Undergoing Fluorodeoxyglucose Positron Emission Tomography/Computed Tomography." *Journal of Clinical Medicine*, **13**(6), p.1575.

[22] Al-Tameemi, M.M.E. and Muslim, R.K., 2024. "Mathematical Modeling Methods for Cancer Tumors a Systematic Review and Comparison Analysis." *Journal of Global Scientific Research,* **9**(7), pp.3581-3592.

[23] Shahzadi, N., Javaid, N., Akbar, M., Aldegheishem, A., Alrajeh, N., & Bouk, SH (2024). "A novel data driven approach for combating energy theft in urbanized smart grids using artificial intelligence." *Expert Systems with Applications,* **253**, 124182.

[24] Khan, ZA, Waqar, M., Chaudhary, NI, Raja, MJAA, Khan, S., Khan, FA, ... & Raja, MAZ (2024). "Fractional gradient optimized explainable convolutional neural network for Alzheimer's disease diagnosis." Heliyon, **10**(20).

[25] Zafar, MM, Javaid, N., Shaheen, I., Alrajeh, N., & Aslam, S. (2025). "Enhancing clinical decision support with explainable deep learning framework for C-section forecasting." *Computing,* **107**(1), 1-45.

[26] Murad, M., Jalil, A., Bilal, M., Ikram, S., Ali, A., Khan, B., & Mehmood, K. (2021). "Radial Undersampling-Based Interpolation Scheme for Multislice CSMRI Reconstruction Techniques." *BioMed Research International*, **2021**(1), 6638588.

[27] Hashim, M., Khan, L., Javaid, N., Ullah, Z., & Javed, A. (2024). "Stacked machine learning models for non-technical loss detection in smart grid: A comparative analysis." *Energy Reports,* **12**, 1235-1253.

[28] Ammar, M., Javaid, N., Alrajeh, N., Shafiq, M., & Aslam, M. (2024). "A Novel Blending Approach for Smoking Status Prediction in Hidden Smokers to Reduce Cardiovascular Disease Risk." *IEEE Access*.

[29] Shaheen, I., Javaid, N., Alrajeh, N., Asim, Y., & Aslam, S. (2024). "Hi-Le and HiTCLe: Ensemble Learning Approaches for Early Diabetes Detection using Deep Learning and eXplainable Artificial Intelligence." *IEEEAccess.*

[30] Alghamdi, TA, & Javaid, N. (2024). "Energy optimization with authentication and cost-effective storage in the wireless sensor IoTs using blockchain." *Computational Intelligence,* **40**(1), e12630.